Generation and Evolution of Natal Pulses: Solitary Meanders in the Agulhas Current

WILHELMUS P. M. DE RUIJTER AND PETER JAN VAN LEEUWEN

Institute for Marine and Atmospheric Research Utrecht, Utrecht University, Utrecht, the Netherlands

JOHANN R. E. LUTJEHARMS

Department of Oceanography, University of Cape Town, Rondebosch, South Africa

(Manuscript received 14 May 1997, in final form 1 February 1999)

ABSTRACT

Solitary meanders of the Agulhas Current, so-called Natal pulses, may play an important role in the overall dynamics of this current system. Several hypotheses concerning the triggering of these pulses are tested using sea surface height and temperature data from satellites. The data show the formation of pulses in the Natal Bight area at irregular intervals ranging from 50 to 240 days. Moving downstream at speeds between 10 and 20 km day^{-1} they sometimes reach sizes of up to 300 km. They seem to play a role in the shedding of Agulhas rings that penetrate the South Atlantic. The intermittent formation of these solitary meanders is argued to be most probably related to barotropic instability of the strongly baroclinic Agulhas Current in the Natal Bight. The vorticity structure of the observed basic flow is argued to be stable anywhere along its path. However, a proper perturbation of the jet in the Natal Bight area will allow barotropic instability, because the bottom slope there is considerably less steep than elsewhere along the South African east coast. Using satellite altimetry these perturbations seem to be related to the intermittent presence of offshore anticyclonic anomalies, both upstream and eastward of the Natal Bight.

1. Introduction

The Agulhas Current is a major western boundary current along the east coast of South Africa. Its water originates from recirculation in a southwest Indian Ocean subgyre, from the Mozambique Channel, and from east of Madagascar (e.g., Gründlingh 1980; Lutjeharms et al. 1981; Seatre and Jorge da Silva 1984; Gründlingh 1992; Lutjeharms 1996). After the Agulhas separates from the curved southern tip of the continent it makes a large anticyclonic turn, approximately conserving its potential vorticity, and flows back east into the southern Indian Ocean as the Agulhas Return Current (Lutjeharms and van Ballegooyen 1988a; Ou and de Ruijter 1986). In this retroflection area large anticyclonic rings are formed, which travel into the South Atlantic Ocean (Boudra and de Ruijter 1986; Olson and Evans 1986; Lutjeharms and Gordon 1987; Gordon and Haxby 1990; Naeije et al. 1992; Feron et al. 1992). These eddies are the largest in the ocean and probably establish a key connection in the global thermohaline circulation, with impact on regional and global climate (Veronis 1973; de Ruijter 1982; Gordon 1986; Gordon et al. 1992).

Compared to other western boundary currents the Agulhas Current adjacent to southern Africa's east coast exhibits a remarkable stability, with very little sideways meandering along the greater part of its trajectory. Gründlingh (1983) has estimated that the current's average path is in fact invariant to ± 15 km. This current path stability between Cape St. Lucia (Fig. 1) and the Agulhas Bank south of Africa is interrupted only at irregular intervals by the passage of large solitary meanders, which have been named ''Natal Pulses'' (Lutjeharms and Roberts 1988). An example is given in Fig. 2, an infrared satellite image.

The observed Natal pulses have some remarkable characteristics. They seem to originate in the region of the Natal Bight (Fig. 1), a distinct offset in the coastline north of Durban. They move downstream at a rate of about 20 km per day (e.g., Gründlingh 1979) and grow steadily in size during this movement. Attempts to identify such pulses in the current north of the Natal Bight have been largely unsuccessful. Similar features may possibly evolve from the Delagoa Bight, a comparable coastal offset farther upstream, but have not been observed to progress downstream (Gründlingh 1992).

The Natal pulse is more than a kinematic curiosity. It has been suggested that it may play a central role in

Corresponding author address: Dr. Peter Jan van Leeuwen, Institution Marine and Atmospheric Research Utrecht, Utrecht University, Post Office Box 80005, 3508 TA Utrecht, the Netherlands.
E-mail: leeuwen@phys.ruu.nl

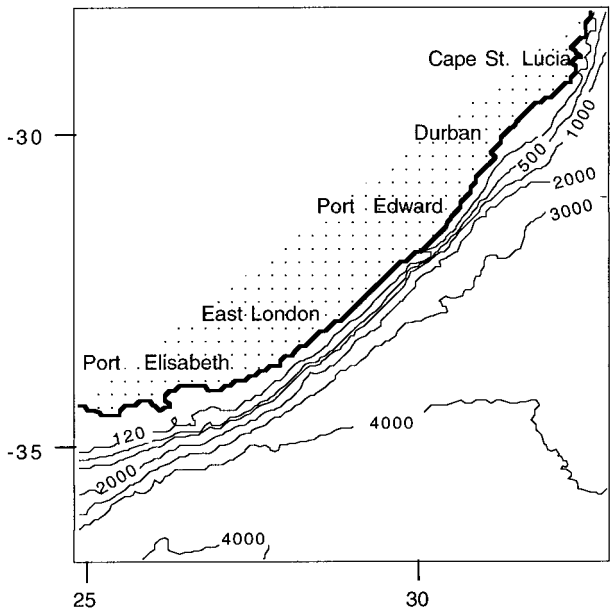

FIG. 1. Bottom topography off the Natal coast.

upstream retroflection of the Agulhas Current (Lutjeharms and van Ballegooyen 1988b) and in the shedding of eddies from the seaward side of this current (Lutjeharms et al. 1992). Such upstream diversions of substantial quantities of water from the Agulhas Current may, in turn, significantly influence the behavior of the downstream Agulhas retroflection, where Agulhas rings are shed to complete the interocean transfer of water from the Indian to the South Atlantic Ocean. Furthermore, the irregular passage of Natal pulses and their embedded cyclonic eddies may cause inshore countercurrents (Lutjeharms and Connell 1989) that carry fish larvae and other organisms upstream along the coast.

The peculiar characteristics of the Natal pulse give rise to a number of questions. What is so special about the Natal Bight that pulses should originate mainly from there? Why do they emerge at irregular intervals; that is, what triggers their initiation? Why do they grow with distance downstream, and are the cyclonic eddies associated with them their cause or effect?

Various mechanisms for the initiation of the meanders have been proposed. It has been observed that the location of the current in the Natal Bight area changes suddenly in coincidence with rising atmospheric pressure following a coastal low (Pearce 1977). However, no significant relationship could be found between winds and meanders of the Agulhas Current. Lutjeharms and Roberts (1988) have mentioned that the meanders could be due to topographically induced, coastally trapped lee eddies, which are driven energetically by the Agulhas Current. Occasionally, these lee eddies may escape as a process of vortex shedding and travel downstream on the inshore side of the Agulhas Current. They also coined the possibility that the adsorption of deep-sea eddies onto the seaward border of the Agulhas Current may act as a triggering mechanism for the formation of a Natal pulse. Gründlingh (1992) has mentioned that sometimes large meanders are formed north of the Natal Bight area as well, possibly due to inherent instability of the flow or to the adsorption of a cyclonic eddy from farther east into the current. Lutjeharms (1989) hypothesized that eddies that have been observed to be spawned at the subtropical convergence to the south (Lutjeharms and Valentine 1988), drift to the north, and interact with the Agulhas Current along the Natal coast, thus triggering a Natal pulse. This would agree with observed seaward disturbances on the Agulhas Current (Lutjeharms and Roberts 1988) and on the Gulf Stream (e.g., Nof 1986).

In this paper the triggering of Natal pulses is investigated using satellite altimeter observations from the Geosat, *ERS-1*, and TOPEX/Poseidon missions, and NOAA satellite infrared imagery. In the next section the satellite observations are described and the identification of Natal pulses is explained. In the following section several of the above described hypothetical mechanisms for Natal-pulse formation are investigated. We find that the most probable generation mechanism is barotropic instability of the baroclinic Agulhas Current. Such an instability may be expected over the relatively flat bottom topography close to Durban, where water columns can move relatively easy up or down slope. Hydrographic cross-shore sections in the Natal Bight carried out in the past are used to check the proposed necessary conditions for instability. It is found that these conditions may be met occasionally. The results are discussed and a concluding section closes the paper.

2. Satellite observations

Three years of Geosat and two years of *ERS-1* and TOPEX/Poseidon altimeter data were processed to search for the generation and the evolution of Natal pulses. Only the first 18 months of Geosat data could be used because of altimeter failure this close to the coast. Also for *ERS-1* some tracks were lost.

The pulses have such small dimension close to Durban (a diameter of about 30 km) that the sea surface topography signals are smoothed away on gridded maps. Therefore individual tracks have been used to estimate the time of their creation. Interpretation of track signals farther from the coast is so difficult that gridded maps were used there.

Infrared imagery from the Pathfinder Project (Vazquez et al. 1994) has been used to validate the altimeter observations. Unfortunately, we could not use the infrared data to follow and study each individual Natal pulse because of persistent cloud cover over the area; only snapshots are available to complement the altimeter results.

FIG. 2. NOAA infrared image. Grayscale from white (cold) to black (warm), with white clouds over land. Two Natal pulses are visible as cyclonic meanders in the relatively dark (warm) Agulhas Current between Durban and Port Elizabeth.

a. Altimeter data analysis

Geosat altimeter data of the period November 1986 to April 1988 have been used for the analysis. Obvious errors were removed and corrections applied for the solid earth and ocean tides, the dry and wet troposphere (from the Fleet Numerical Oceanography Center), the inverse barometer effect, and the sea state bias (2% of the significant wave height). The mesoscale ocean signal was derived from the corrected altimeter heights using collinear track analysis as described in Feron et al. (1992). A sinusoidal radial orbit error removal was applied (see, e.g., Wakker et al. 1990). The resulting sea surface heights show only the time-varying part of oceanic features, after the time mean has been subtracted. Note that the time mean consists of the unknown time-mean currents and the unknown geoid.

ERS-1 and TOPEX/Poseidon data for the period of April 1992 until December 1994 have been processed as well. The mesoscale ocean signal was derived from corrected altimeter heights using crossover minimalization with a Fourier series model up to degree 2 (Wisse et al. 1995).

To identify Natal pulses individual arcs were used covering the East African coastal zone (see Figs. 3a and 3b). Being cyclonic events, Natal pulses show up as depressions in the time-variable surface topography. Examples for Geosat are given in Fig. 4. The anomaly in track 275 could be identified as the Natal pulse observed

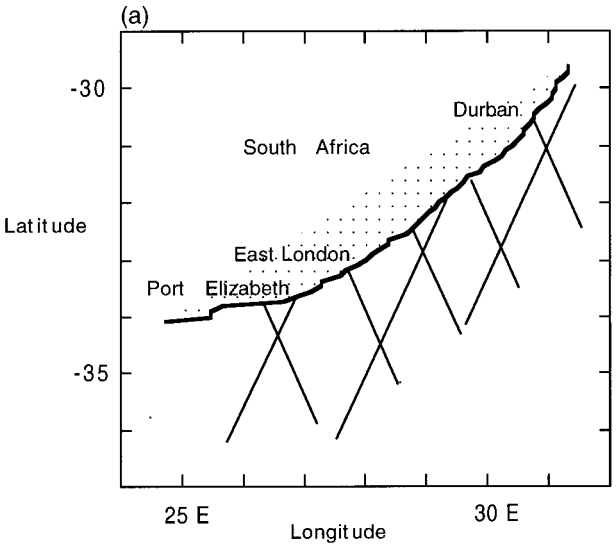

FIG. 3a. Geosat ground tracks used in the collinear-track analysis: D is Durban, EL is East London, and PE is Port Elizabeth.

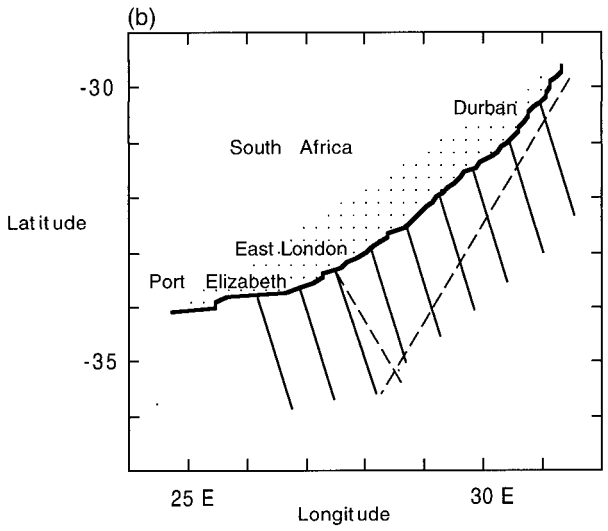

FIG. 3b. *ERS-1* (solid) and TOPEX/Poseidon (dashed) ground tracks used in the collinear-track analysis: D is Durban, EL is East London, and PE is Port Elizabeth.

by Gründlingh (1992) from a NOAA infrared image (Fig. 2).

To identify their origin in the Natal Bight area, distance-weighted interpolation was used to produce 0.5° by 0.5°, weekly interpolated maps for Geosat. The combined *ERS-1* and TOPEX/Poseidon dataset was interpolated to the same grid, every 10 days. The interpolation was a Guassian weighting in space and time, with decorrelation lengths of 0.5°, 7 days for Geosat and 0.5°, 10 days for *ERS-1* and TOPEX/Poseidon. It produced visually the same results as collocation. (Figures 9a–d show examples of sea surface topography anomaly maps in the Natal Bight area. These are discussed in section 4.)

b. Identification of Natal pulses

From earlier analysis of infrared images and hydrographic data (Lutjeharms and Roberts 1988; Gründlingh 1992) a Natal pulse is characterized by the following properties:

- it manifests itself as a cyclonic eddy in the current
- it spawns close to Durban
- it travels in the downstream direction with a velocity of 10–20 km day^{-1}
- its diameter ranges from 30 to 200 km
- it follows the Agulhas Current along the east coast of South Africa.

All tracks in the examined period were explored for cyclonic features. Only those were selected with an amplitude of at least 10 cm and a width of at least 30 km in order to prevent noise and other small-scale features to blur the picture. In Figs. 5a and 5b the results are depicted for Geosat and *ERS-1*/TOPEX/Poseidon, respectively. Each track is represented by a single character. A track with a cyclonic feature is depicted in the figures as an ○. A track without such feature is depicted with a small ×. The observed cyclonic features have diameters in the correct range (see Fig 4). Their height amplitudes varied from 10 cm to over 1 m. This variation in magnitude can be related to growth of the pulses, to the satellite ground track crossing the edge of a pulse or to pulses having different sizes. Also indicated (by squares) in Fig. 5 are thermal infrared observations of Natal pulses (clouds permitting). They give extra support to the altimeter data analysis.

Dotted lines in Figs. 5a and 5b denote possible paths of the features along the coast. In total 14 events are visible that can be identified with Natal pulses. They appear to travel downstream with velocities of 10–20 km day^{-1} agreeing with estimates obtained from satellite infrared images (Lutjeharms and Roberts 1988). A strong increase in the number of meanders is observed near East London, around 600 km downstream from Durban, and beyond. This is probably due to the widening of the continental shelf at that point, allowing a more unstable current there. Figures 5a and 5b show that occasionally more than one pulse is present in one ''event'' denoted by the dotted lines. This phenomena was confirmed by the infrared images.

Pulses, or pulse events, appear to be formed mostly intermittently with a period between 50 and 150 days. However, in the first nine months in 1993, no Natal pulses could be identified at all. Apparently, longer timescale variations exists in pulse formation.

3. Analysis of suggested triggering mechanisms

After having identified the Natal pulses from individual tracks we have tried to identify their triggering

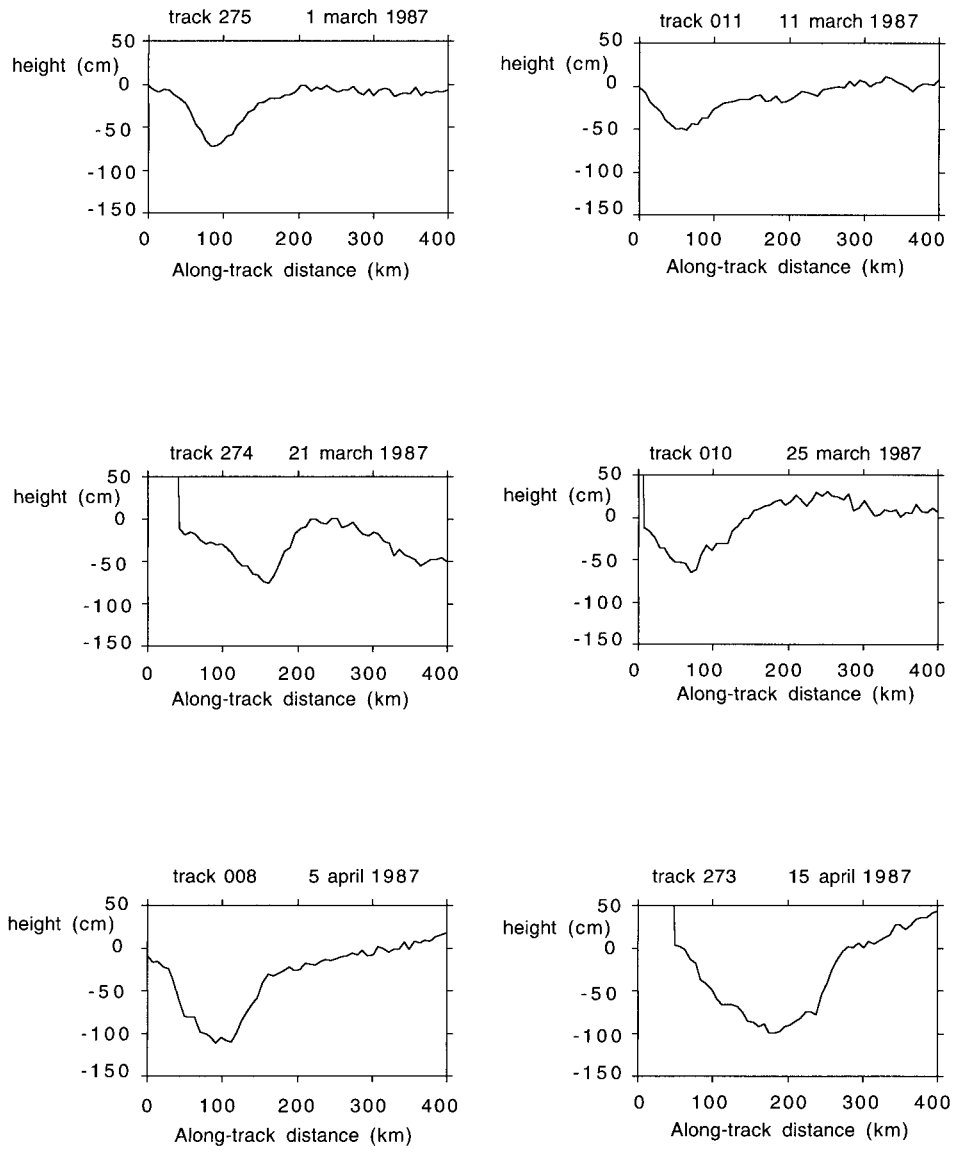

FIG. 4. Individual profiles from Geosat tracks with dates as indicated for the same Natal pulse travelling along the coast. Note the increase in strength as the pulse travels south.

mechanism from interpolated spatial images of sea height anomaly. Four possible processes have been examined.

a. Triggering by eddies pinched off from the meandering Agulhas Return Current/Subtropical Convergence

Such eddies were speculated to move in a northwestward direction until hitting the Agulhas Current, possibly inducing large meanders in it (Lutjeharms 1989). To investigate this, travel paths of anomalies were examined from the sea-height anomaly fields. In general, eddies pinched off from the strongly meandering Agulhas Return Current appeared to travel westward to feed back into this current (see also Feron et al. 1998 and Gründlingh 1995). Some eddies were lost in the altimeter signal. No eddy, cyclonic or anticyclonic, was observed to cross the area from the Agulhas Return Current to the Agulhas when the latter still flows along the coast of South Africa. So, this suggestion is not supported by the altimeter data.

b. Generation by lee eddies escaping from the Natal Bight

While the Agulhas flows along the Natal Bight, a relatively shallow cyclonic lee eddy is formed in the

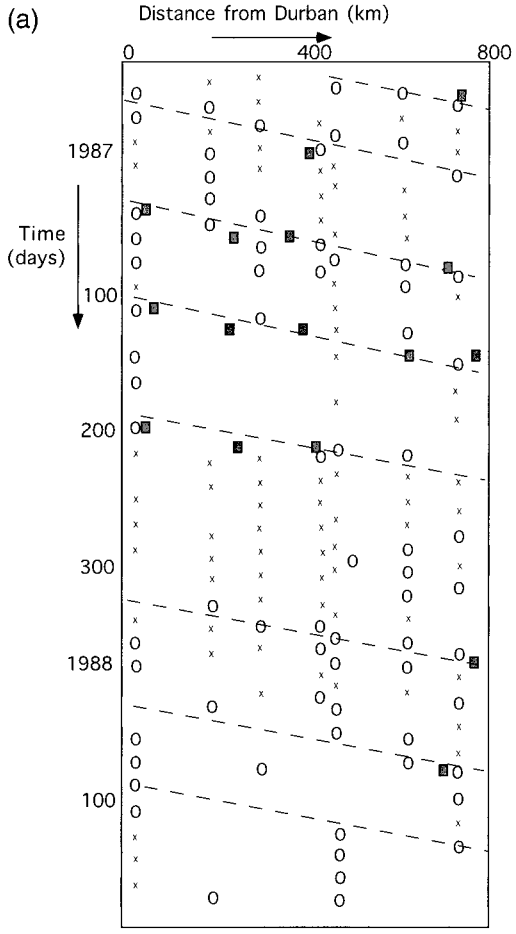

FIG. 5a. Identification of Natal pulses with Geosat. Open circles denote cyclonic anomalies, crosses no significant feature, and the absence of a character bad tracks. Gray squares denote infrared observations of a Natal pulse. The dashed lines show the possible propagation of a Natal pulse (or of a pair of pulses).

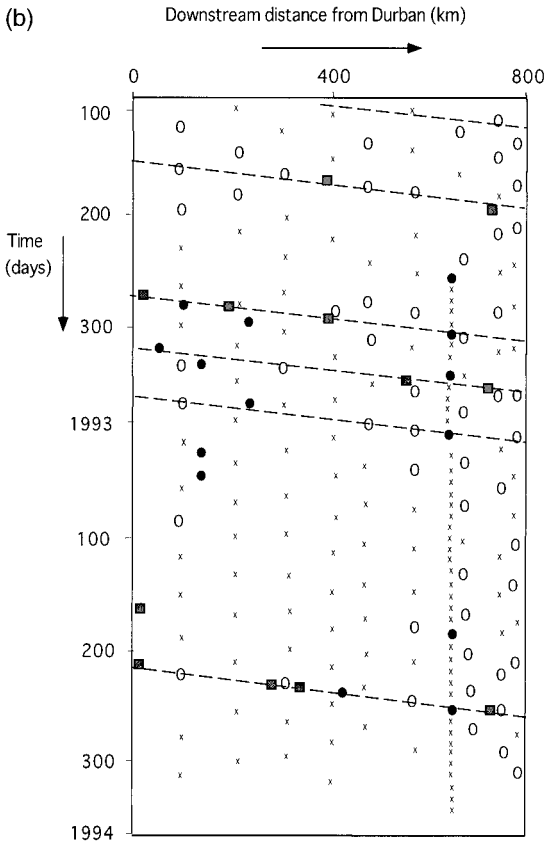

FIG. 5b. Identification of Natal pulses with *ERS-1* and TOPEX/Poseidon. Open circels denote cyclonic anomalies of ERS-1, black circles denote cyclonic anomalies of TOPEX/Poseidon, crosses no significant feature, and the absence of a character bad tracks. Gray boxes denote infrared observations of a Natal pulse. The dashed lines show the possible path of a Natal pulse (or of a pair of pulses).

bight (e.g., Pearce 1977; Lutjeharms and Roberts 1988; see also Gill and Schumann 1979). Every now and then this eddy might become so strong that it is shed from the bight, producing a solitary meander in the Agulhas, which is then transported south along the coast. For this process to be true relatively strong cyclonic eddies should be observed in the Natal Bight, followed by an anticyclonic signal at escape. However, the Geosat track that crosses this area showed a strong cyclonic feature only once, in the first repeat orbit. This track seems to be reliable in the Natal Bight region in 75% of the cases for longer periods of time, so a strong signal had to be visible, if present. Another Geosat track does show cyclonic features north of Durban, but only in two cases did it precede a Natal pulse, while in five cases it did not. This means that the lee eddy escaping from the bight gives no significant surface signal. But then it is unlikely to perturb the Agulhas Current significantly. Either way, there is no clear evidence for this mechanism from the altimeter data analysis.

c. Adsorption of deep-sea cyclonic eddies

These eddies seem to originate from east of Madagascar (Lutjeharms 1989; Gründlingh et al. 1991; Lutjeharms and Roberts 1988; Gründlingh 1992). Close examination of the gridded fields did not show the adsorbtion of cyclonic features into the Agulhas. Also Gründlingh (1995) found no evidence for adsoption in his analysis of the first year of TOPEX/Poseidon data (see his Fig. 11). All features seemed to stay at least about 100 km from the coast, sometimes moving along at the seaward edge of the Agulhas (Gründlingh 1995). On a few occasions in the full dataset part of a large cyclonic system upstream of Cape St. Lucia seemed to be adsorbed by the current. However, such an interaction leads to the generation of a Natal pulse only if accompanied by an anticyclonic feature east of Durban (see section 4 and also Fig. 10 for examples). Clearly, the Agulhas itself in that area is highly variable and not well defined, so perhaps these features form part of the varying upstream branches feeding into the Agulhas, which are still largely unknown (Lutjeharms 1996; de

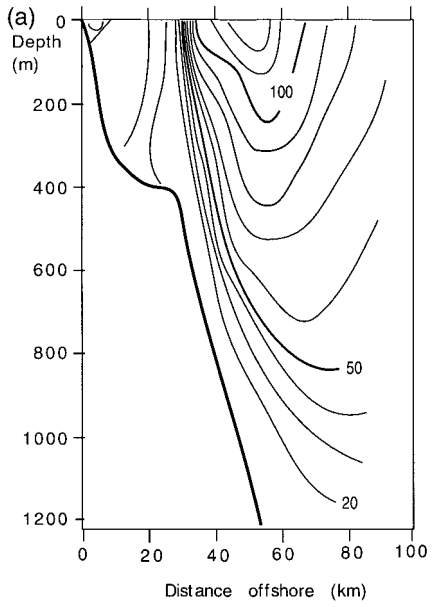

FIG. 6a. Averaged velocity section near Durban, after Toole and Raymer (1985). Contour interval 10 cm s^{-1}.

Ruijter et al. 1999). It is not an adsorption in a well-defined current. The necessary presence of anticyclonic features for Natal pulse generation is analyzed further in section 4.

d. Instability of the Agulhas

To investigate the possibility that Natal pulses are formed due to an instability of the Agulhas Current, conditions for linear stability of the current have been determined. Such an analysis is complicated by the marked horizontal and vertical structure of the current and the large bottom slope (see Fig. 6). To first order the momentum balance is semigeostrophic in this area (e.g., Ou and de Ruijter 1986), with geostrophy only in the alongshore component. Consequently, earlier studies based on the quasigeostrophic approximation (e.g., Charney and Stern 1962, Pedlosky 1964, 1970, 1987; Blumen 1968; Hart 1974; de Szoeke 1975; Killworth 1980; Steinsaltz 1987; Samelson and Pedlosky 1990) cannot be applied directly.

It can be shown that the time evolution of the sum E of the kinetic and potential energy of a perturbation on a semigeostrophic jet is given by

$$\frac{\partial E}{\partial t} = \iint \overline{u}_y uv \, dy \, dz + \iint \frac{gf}{\rho_0 N^2} \overline{u}_z v\rho \, dy \, dz \equiv \text{TKE} + \text{TAPE}. \quad (1)$$

TKE and TAPE denote the transfer of energy from the mean flow to the perturbations, feeding on the kinetic or available potential energy of the mean flow, respectively. Here the x coordinate is chosen along the current axis southwestward and the y coordinate positive seaward across the current; $\overline{u}(y, z)$ is the mean current of which the stability is investigated, u and v are the perturbation velocities, f is the planetary vorticity, ρ is the perturbation density, ρ_0 is the mean density, and N is the buoyancy frequency, defined by $N^2 = g(\log\overline{\rho})_z$.

An order of magnitude estimate for the energy transfer terms can be obtained from observations of the basic current structure. Toole and Raymer (1985) have constructed an averaged section of southward alongshelf velocity in the Agulhas Current off Durban (Fig. 6a) from repeated hydrographic measurements taken mainly during the late 1960s and early 1970s (e.g., Pearce 1977). For the inshore edge of the Agulhas Currrent the cross-shore scale is about 10 km, while $\overline{u}$ varies nearly linearly with depth, with a proportionality constant of about -1.2×10^{-3} s^{-1} (Fig. 6a); f^2/N^2 is estimated from Houry et al. (1987) as 5.3×10^{-5} (a conservative estimate). If we take the horizontal and vertical scale of the perturbation equal to that of the mean velocity and use geostrophy, we find TKE/TAPE $\approx (N^2/f^2)\, l_z^2/l_y^2 \approx 140$, indicating that instabilities, if arising, can be expected to be mainly barotropic.

This is different for other western boundary currents. For instance, the Gulf Stream becomes mixed or baroclinically unstable. In Fig. 6b a geostrophic velocity profile is given as representative for the Gulf Stream in the South Atlantic Bight (from Miller and Lee 1995). A characteristic horizontal length scale is 20 km, a ver-

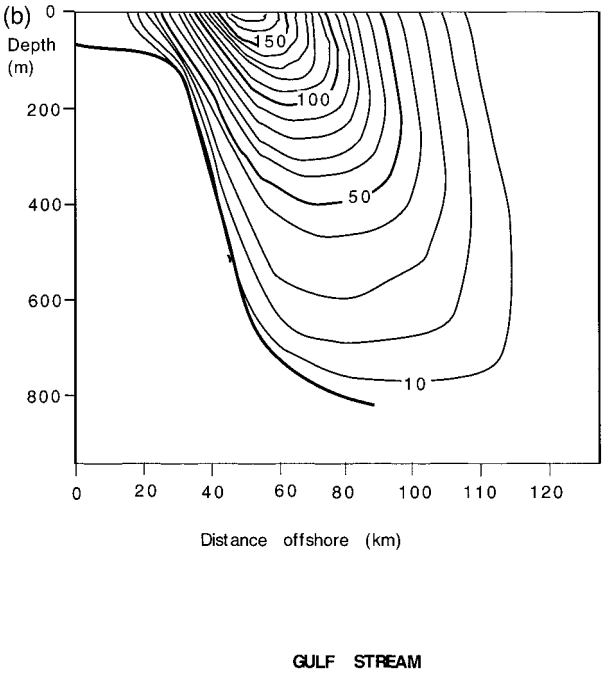

FIG. 6b. Averaged velocity section for the South Atlantic Bight after Miller and Lee (1995). Contour interval, 10 cm s^{-1}.

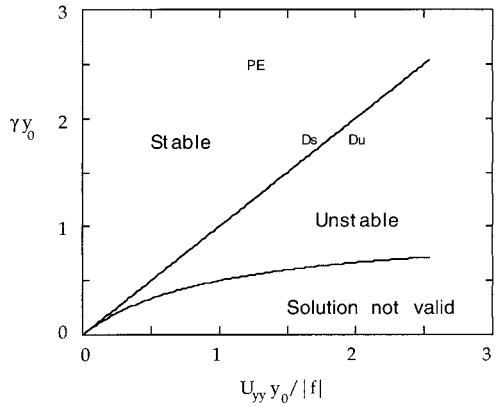

FIG. 7. Stability diagram of normalized bottom slope versus normalized jet steepness. The two lines mark the unstable regime. The mean flow at Durban (Ds) is stable, but a slight increase in sharpness results in an unstable current (Du). The current is stable at Port Edwards (PE).

tical shear of $\overline{u}_z$ about 4.0×10^{-1} s^{-1}; f^2/N^2 is estimated from Levitus (1982) as about 1.4×10^{-4}. With the same assumptions on the perturbations as above we now arrive at TKE/TAPE ≈ 4.5. So, the Gulf Stream is likely to be more sensitive to mixed instabilities. The reason for this striking difference is that the Gulf Stream is broader, more stratified, and more confined to the upper layers than the Agulhas.

Next step is to check whether a necessary condition for barotropic instability, which is a vorticity constraint related to cross-stream (and cross topographic) meandering, can be fulfilled in the Natal Bight area. A necessary condition for instability of a baroclinic current in a continuously stratified fluid over a sloping bottom is derived in the appendix. The derivation is slightly complicated because the relative vorticity of the basic current is comparable in magnitude to the planetary vorticity. For the Agulhas Current it boils down to the condition that, at least at a certain depth z_{cr} and cross-current position y_{cr}, the lateral potential vorticity gradient changes sign:

$$\left(\frac{f - \overline{u}_y}{h}\right)_y = 0 \quad \text{for } y = y_{cr}, \qquad z = z_{cr}. \tag{2}$$

This condition has the same form as the necessary condition for barotropic instability in a *barotropic* fluid

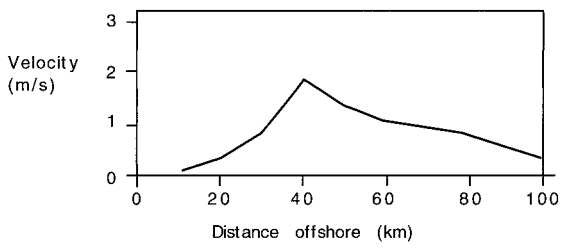

FIG. 8. Averaged velocity profile near Durban over the upper 100 m, after Pearce (1977).

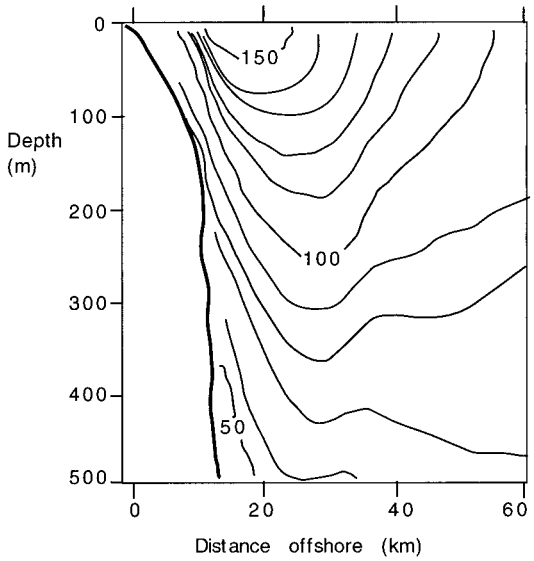

FIG. 9. Averaged velocity section near Port Edward, after Pearce (1977). Contour interval: 10 cm s^{-1}.

(e.g., Pedlosky 1987; Le Blond and Mysak 1978) except that now the condition has to be met by the baroclinic current somewhere in the jet.

To apply the above to the Agulhas Current we restrict ourselves to the region with the largest horizontal gradients, between $y = 20$ km and $y = 35$ km. The velocity profile and the bottom profile can be approximated by $\overline{u}(y, z) = \alpha(z)y^2$ ($\alpha > 0$, $0 < y < y_0$) and $h(y) = h_0 e^{\gamma y}$ ($h_0 > 0$, $\gamma > 0$), in which we choose $y = 0$ at 20 km from the coast and $y_0 = 15$ km. Note that α is maximal in the upper 100 m (see Fig. 6a). Substitution in (2) gives as a necessary condition for instability: $y_{cr} = 1/\gamma + f/\alpha(z)$. The condition $0 \leq y_{cr}$ finally leads to

$$\frac{\overline{u}_{yy} y_0}{|f|} > \gamma y_0. \tag{3}$$

For fixed maximum horizontal shear gradient [$\overline{u}_{yy} = 2\alpha(z)$] condition (3) is easier satisfied if the bottom slope is gentler (i.e., if γy_0 becomes smaller). For a given slope (γ fixed) a sharper jet [i.e., larger $\alpha(z)$] favors the condition. The condition $y_{cr} \leq y_0$ is of no physical importance but only indicates to what distance the approximations for $\overline{u}$ and h are valid.

We estimate (see Fig. 6a) $\alpha(0) = 4.0 \times 10^{-9}$ m^{-1} s^{-1} and $\gamma = 1.2 \times 10^{-1}$ m^{-1}. In Fig. 7 this point is depicted in the stability diagram with character "**Ds**," of Durban. It lies just within the stable regime but is close to instability. In fact, an increase in jet sharpness with only a factor 1.2 is enough to push the point in the unstable area, denoted by "**Du**" in Fig. 7. Individual observed profiles indicate that this criterion is met occasionally (Fig. 8).

When applying the above farther downstream, the continental slope is so steep that barotropic instabilities cannot be triggered. For instance, near Port Edward (Fig.

9) the inshore edge of the jet may be characterized by $\alpha = 1.0 \times 10^{-8}$ and the very steep topography by $\gamma = 5.0 \times 10^{-4}$ m^{-1}. A value for y_0 of 5 km, denoted by "**PE**" in Fig. 7, shows that at this location the current is far from barotropic instability.

Our conclusion is that the "average" Agulhas Current is stable along the continental slope. Occasionally, however, the actual current is stronger and its profile sharper in the Natal Bight area so that the necessary condition for barotropic instability is satisfied. This probably results in a growing meander, which may evolve to a Natal pulse.

4. Discussion

Analysis of satellite altimeter and infrared data support the hypothesis that Natal pulses start as topographically induced instabilities, triggered by an increase in strength and sharpness of the Agulhas Current close to Durban, where the topographic slope relaxes in the Natal Bight. If that conclusion is correct, then the question arises what the causes for such increases in the jet might be, particularly since the occurrence of Natal pulses is highly irregular. To this end we examined gridded sea-surface height anomaly fields of the area offshore of the Natal Bight.

A Natal pulse is expected when the Agulhas increases its horizontal shear upstream of Durban. This can be achieved by a large antiyclonic anomaly seaward of the upstream Agulhas (Fig. 10). Tables 1 and 2 show that the aforementioned situation indeed precedes a Natal pulse. The first column gives the date at which an anticyclonic anomaly moves within 200 km of the Natal Bight. The second column indicates the structure and position of the anomaly field at that instant, and the third column shows the date at which a Natal pulse emerges, as derived from the individual tracks in Fig. 5. The fact that the days of observation in the first and the third column are not precisely the same might be due to the uncertainties in the time estimates: the gridded fields are interpolated weekly (Geosat) and every ten days (*ERS-1* and TOPEX/Poseidon), and the actual beginning of the Natal pulse can only be obtained with an uncertainty of 17 days (the repeat period of Geosat) or 10–35 days for the other satellites. So a mismatch of up to about 17, respectively 35, days can be accounted for. The tables suggest a relation between the presence of anticyclonic anomalies and the generation of Natal pulses. Occasionally, a cyclone may be present northeast of Durban just before the appearance of a Natal pulse, but certainly not in all cases.

The anticyclonic anomalies originate from farther east and northeast. They seem to have their influence on the Natal Bight area, after which they move either south into the Agulhas Return Current region or they weaken and finally disappear from the images. Sometimes an anomaly moves eastward, away from the Natal Bight area, to return later, at which a new Natal pulse appears. Unfortunately, the size and propagation of the anomalies in this part of the ocean is so erratic that a more conclusive analysis like that leading to Fig. 5 could not be performed in this case.

The picture that emerges is the following: Large cyclonic and anticyclonic anomalies from the east and northeast perturb the outer edges of the Agulhas. Anticyclonic features favor an increase in current strength upstream of Durban. This increase in strength might trigger barotropic instability of the baroclinic current, which is possible here due to the relatively small bottom slope. The instability evolves into a Natal pulse. It is important to note that Figs. 5a and 5b do not show the generation of pulses farther south, where large offshore anomalies sometimes influence the current as well. This was also found from infrared images (Lutjeharms and Roberts 1988) and is most probably due to the slope topography that is much steeper there. It seems clear that the relatively small bottom slope close to Durban is indeed a necessary condition for their formation. A stability analysis of FRAM (Fine Resolution Antarctic Model) has shown that instabilities in the model are mainly baroclinic, but it is mainly barotropically unstable near Durban (Ivchenko et al. 1997). These findings add support to our observations and hypothesis. Of course, it is difficult to access the amplitude of the disturbance by these anomalies, so it is difficult to predict if a *linear* stability analysis will already show Agulhas instability. Currently, we are performing a more complete stability analysis using a numerical model.

5. Conclusions

The generation of Natal pulses, large solitary meanders in the Agulhas Current originating in the Natal Bight area, has been shown to be most probably related to barotropic instability of the baroclinic current in that area. The steepness of the continental slope is much less in this area than elsewhere along the southeast African coast, thus favoring meander growth. Support for this hypothesis has been obtained both from hydrographic and satellite altimeter data.

We identified six Natal pulses from analysis of individual tracks of 18 months of Geosat altimeter data. Two years of combined *ERS-1* and TOPEX/Poseidon data revealed eight Natal pulses. Most findings were accompanied by one or more infrared identifications. The pulses appeared at irregular intervals, sometimes in pairs. Their average propagation speed is about 15 km day^{-1}, in close agreement with earlier estimates based on satellite infrared images of sea surface temperature (Lutjeharms and Roberts 1988).

Analysis of gridded satellite altimeter data suggested that the formation of a Natal pulse is accompanied by anticyclonic features east of Durban. These eddies originate from farther east or from the Mozambique Channel. The anomalies seem to perturb and enhance the

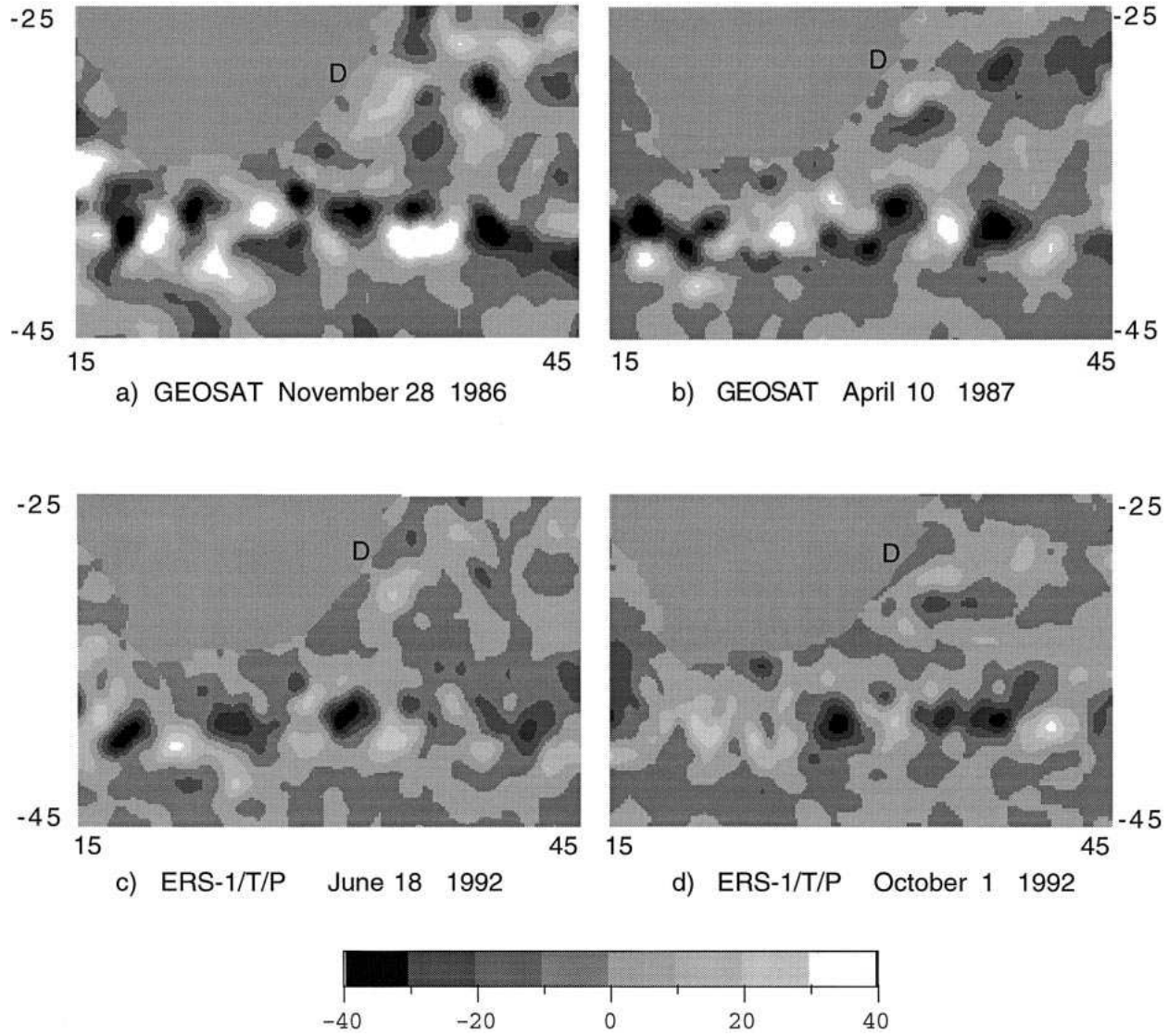

FIG. 10. Examples of gridded anomaly fields south and east of the African continent. Anticyclonic anomalies are white, cyclonic anomalies are dark, contour interval is 10 cm, D is Durban. In all cases an anticyclonic anomaly lies east of Durban, with a weaker anomaly on its inshore side. This indicates an increasing strength and sharpness of the Agulhas Current, probably triggering a Natal pulse.

basic current so that instabilities can grow and Natal pulses are generated.

The stability analysis of the Agulhas Current is complicated by its large relative vorticity, which is of the order of the planetary vorticity. This means that perturbations are not in geostrophic balance. However, the altimeter and hydrographic observations suggest that to first order the alongstream velocity is geostrophic, while the cross-stream velocity is not. Using this approach we found that for an ''average'' Agulhas Current the maximum speed and cross-shore profile of the current are such that the necessary condition for barotropic instability is not met in the Natal Bight. At other locations the bottom slope is so steep that the basic flow is very stable. However, the necessary condition for instability is close to being satisfied near Durban so that, if maximum speeds are larger or the jet a little sharper, the threshold is exceeded and an instability can grow. Observed Agulhas Current profiles off Durban (e.g., Pearce 1977) show that the variability at that location is large enough to sometimes overcome the stabilizing effect of the topographic slope. However, it is unclear at this stage whether disturbances in the current related to the anomalies offshore can be treated with a linear stability analysis.

A suggested relation between Natal pulses and the shedding of Agulhas Rings in the retroflection region has been investigated by van Leeuwen et al. (1999).

TABLE 1. Relation between observed Natal pulses and large offshore anomalies in the Natal Bight area from Geosat gridded maps. According to our conjecture, a pulse is possible when the position of the offshore features is such that the Agulhas Current increases in strength upstream of Durban.

Date of anomaly arrival east of Durban	Nature of anomalies offshore of Durban	Date of Natal pulse observation
1986:328	Anticyclone east of Durban	1986:330
1987:38	Anticyclone east, cyclone northeast of Durban	1987:40
1987:108	Anticyclone east of Durban	1987:100
1987:197	Anticyclone east, cyclone northeast of Durban	1987:195
1987:304	Anticyclone east, cyclone northeast of Durban	1987:320
1988:14	Anticyclone east of Durban	1988:25

TABLE 2. As in Table 1 but now from *ERS-1* and TOPEX/Poseidon altimeter data.

Date of anomaly arrival east of Durban	Nature of anomalies offshore of Durban	Date of Natal pulse observation
1992:170	Anticyclone east, cyclone northeast of Durban	1992:160
1992:260	Anticyclone east of Durban	1992:280
1992:320	Anticyclone east of Durban	1992:315
1993:10	Anticyclone east, cyclone northeast of Durban	1992:350
1993:90	Weak anticyclone east of Durban	no pulse
1993:210	Anticyclone east of Durban	1993:210

They found that some pulses seem to cause a shedding themselves, while others interact with Rossby waves in the Agulhas Return Current to form Agulhas Rings.

Acknowledgments. We thank the anonymous reviewers for several constructive remarks that led to a much better paper. W. P. M. de Ruijter thanks Prof. Lutjeharms and Prof. Brundrit for inviting him for a ''mini sabbatical'' to the University of Cape Town, during which this study was initiated. Discussions with the Physical Oceanography Group at UCT were very stimulating. This research was sponsered by the Space Research Organization Netherlands, under Grant EO-002, and the ''National Research Program'' NOP II, Grant 013001237.10 (PJVL and WPMR). The research by JREL was funded by the South African Foundation for Research Development and by the Department of the Environment as part of its contribution to WOCE. R. C. V. Feron from IMAU and M. C. Naeye from the Delft University of Technology, Section for Space Research and Technology, are gratefully acknowledged for their continued support with the Geosat data and the combined *ERS-1* TOPEX/Poseidon data, respectively.

APPENDIX

Instability Condition

In this appendix we derive a necessary condition for instability. A characteristic velocity scale is $U = 1$ m s^{-1} (see Fig. 6a). We assume that the perturbations have the same cross-current length scale $L_y = 10$ km as the mean profile. The alongshore length scale $L_x = 50$ km of the perturbations can be estimated from altimeter observations of Natal pulses (see Fig. 4). The timescale is chosen to be advective $T = L_x/U$. We then find for the mean velocity $\overline{u}$ and for the perturbations, to first order,

$$\begin{aligned} \rho_0 f \overline{u} &= -\overline{p}_y \\ \rho_0 f u &= -p_y \\ -\rho_0 (f - \overline{u}_y) v &= -p_x \\ g\rho &= -p_z \end{aligned} \tag{A1}$$

with free-slip boundary conditions at upper and lower boundaries.

A necessary condition for instability can be derived following Pedlosky (1987), but using (A1) instead of quasigeostrophy. Using a normal-mode assumption for the perturbations $p = p(y, z) \exp ik(x - ct)$, we obtain

$$\int_0^{y_0} \int_{-h}^{0} |p_y|^2 + k^2 \frac{f}{f - \overline{u}_y} |p|^2 + \frac{f(f - \overline{u}_y)}{N^2} |p_z|^2 \, dz \, dy$$
$$= \int_0^{y_0} \int_{-h}^{0} \frac{f}{f - \overline{u}_y} \overline{\Pi}_y \frac{|p|^2}{\overline{u} - c} - \frac{f}{N^2} \left[\frac{\overline{u}_y}{\overline{u} - c} \right]_z (\overline{u} - c) p_z p^* \, dz \, dy + \int_0^{y_0} \frac{f(f - \overline{u}_y)}{N^2} p_z p^* \Big|_{-h}^{0} dy \tag{A2}$$

in which the horizontal gradient of the potential vorticity is given by

$$\overline{\Pi}_y = -\overline{u}_{yy} - (f - \overline{u}_y)^2 \left(\frac{f}{N^2} \frac{\overline{u}_z}{f - \overline{u}_y} \right)_z . \tag{A3}$$

This expression differs from its quasigeostrophic analogue only in the presence of the $(f - \overline{u}_y)$ factors.

To proceed, this expression is simplified by investigating the order of magnitude of the different terms. Taking the same characteristic scales as in section 3d,

we find that the second term on the right-hand side of (A2) is about a factor 10 smaller than the potential vorticity term. Furthermore, the cross-current potential vorticity gradient can be approximated by $-\overline{u}_{yy}$. The upper boundary term is proportional to $\overline{u}_z$ and is also an order of magnitude smaller than the other terms. At the lower boundary only the bottom-slope term remains due to its large magnitude: $h_y \approx 0.03$ (Fig. 6a) compared to the isopycnal slope. Following Charney and Stern (1962) we concentrate now on the imaginary part of (A2), leading to the following necessary condition for instability:

$$\int_0^{y_0}\left[\int_{-h}^{0}\frac{|p|^2}{|\overline{u}-c|^2}\frac{f\overline{u}_{yy}}{f-\overline{u}_z}dz+\int_0^{y_0}fh_y\frac{|p|^2}{|\overline{u}-c|^2}\right]dy=0. \tag{A4}$$

This equation expresses transparently that the vorticity structure of the basic current has to be appropriate to overcome the stabilizing effect of the stretching of the water column over the bottom slope. In order to reach this balance the steering level [the level at which $\overline{u} = \mathrm{Re}(c)$, see Pedlosky, 1987] has to be close to the lower boundary. This means that the factor $|\overline{u} - c|^2$ will be close to its minimum value near the lower boundary (see Johns 1988). Because $\overline{u}$ is decreasing with depth and the phase velocity of the perturbations is constant with depth, $|\overline{u} - c|^2$ will attain its maximum near the sea surface.

From calculations presented in the literature (for instance Gill et al. 1974; Johns 1988) one would expect that $|p|^2$ will attain its maximum values close to the pycnocline. If we now assume that perturbations satisfy (A4) for which $|p|^2$ has approximately the same vertical structure as $|\overline{u} - c|^2$ (which is not a strong point in the present analysis, but we are only searching for a necessary condition), we arrive at

$$\int_0^{y_0} b\left[\int_{-h}^{0}\frac{f}{f-\overline{u}_y}\overline{u}_{yy}\,dz+fh_y\right]dy=0 \tag{A5}$$

in which b is the proportionality factor between $|p|^2$ and $|u - c|^2$ (which can still be y dependent). Equation (A5) yields as a necessary condition for instability that the expression between brackets changes sign in the cross-current direction, hence, after some rewriting,

$$\int_{-h}^{0}\frac{f}{f-\overline{u}_y}\left(\frac{f-\overline{u}_y}{h}\right)_y dz=0 \quad \text{for a } y=y_{\mathrm{cr}}. \tag{A6}$$

If the jet is not extremely sharp so that the absolute vorticity $f - \overline{u}_y$ does not change sign, a necessary condition for instability emerges that, at least at a certain depth z_{cr} and cross-current position y_{cr}, the lateral potential vorticity gradient changes sign:

$$\left(\frac{f-\overline{u}_y}{h}\right)_y=0 \quad \text{for } y=y_{\mathrm{cr}}, \qquad z=z_{\mathrm{cr}}. \tag{A7}$$

REFERENCES

Blumen, W., 1968: On the stability of quasi-geostrophic flow. *J. Atmos. Sci.*, **25,** 929–931.

Boudra, D., and W. P. M. De Ruijter, 1986: The wind-driven circulation of the South Atlantic–Indian Ocean 2. Experiments using a multi-layer numerical model. *Deep-Sea Res.*, **33,** 447–482.

Charney, J. G., and M. E. Stern, 1962: On the stability of internal baroclinic jets in a rotating atmosphere. *J. Atmos. Sci.*, **19,** 159–172.

de Ruijter, W. P. M., 1982: Asymptotic analysis of the Agulhas and Brasil Current systems. *J. Phys. Oceanogr.*, **12,** 361–373.

——, A. Biasoch, S. S. Drijfhout, J. R. E. Lutjeharms, R. Matano, T. Pichevin, P. J. van Leeuwen, and W. Weijer, 1999: Dynamics, estimation and impact of the South Atlantic inter-ocean exchange. *J. Geophys. Res.*, in press.

de Szoeke, R. A., 1975: Some effects of bottom topography on baroclinic instability. *J. Mar. Res.*, **37,** 93–122.

Feron, R. C. V., W. P. M. de Ruijter, and D. Oskam, 1992: Ring shedding in the Agulhas Current system. *J. Geophys. Res.*, **97,** 9467–9477.

——, ——, and P. J. van Leeuwen, D. B. Boudra, and E. P. Chassignet, 1998: A new method to determine the mean sea surface dynamic topography from satellite altimeter observations. *J. Geophys. Res.*, **103,** 1343–1362.

Gill, A. E., and E. H. Schumann, 1979: Topographically induced changes in the structure of an inertial coastal jet: Application to the Agulhas Current. *J. Phys. Oceanogr.*, **9,** 975–991.

——, J. S. A. Green, and A. J. Simmons, 1974: Energy partition in the large-scale ocean circulation and the production of mid-ocean eddies. *Deep-Sea Res.*, **21,** 499–528.

Gordon, A. L., 1986: Interocean exchange of thermocline water. *J. Geophys. Res.*, **91,** 5037–5046.

——, and W. F. Haxby, 1990: Agulhas eddies invade the South Atlantic: Evidence from Geosat altimeter and shipboard conductivity–temperature–depth survey. *J. Geophys. Res.*, **95,** 3117–3125.

——, R. F. Weiss, W. M. Smethie, and M. J. Warner, 1992: Thermocline and intermediate water communication between the South Atlantic and Indian Oceans. *J. Geophys. Res.*, **97,** 7223–7240.

Gründlingh, M. L., 1979: Observation of a large meander in the Agulhas Current. *J. Geophys. Res.*, **84** (C7), 3776–3778.

——, 1980: On the volume transport of the Agulhas Current. *Deep-Sea Res.*, **27,** 557–563.

——, 1983: On the course of the Agulhas Current. *S. Afr. Geogr. J.*, **65,** 49–57.

——, 1992: Agulhas meanders: Review and a case study. *S. Afr. Geogr. J.*, **74,** 19–28.

——, 1995: Tracking eddies in the southeast Atlantic and southwest Indian oceans with TOPEX/POSEIDON. *J. Geophys. Res.*, **100,** 24 977–24 986.

——, R. A. Carter, and R. C. Stanton, 1991: Circulation and water properties of the southern Indian Ocean, spring 1987. *Progress in Oceanography*, Vol. 28, Pergamon Press, 305–342.

Hart, J. E., 1974: On the mixed stability problem for quasi-geostrophic ocean currents. *J. Phys. Oceanogr.*, **4,** 349–356.

Houry, S., E. Dombrowsky, P. de Mey, and J.-F. Minister, 1987: Brünt–Väisalä frequency and Rossby radii in the South Atlantic. *J. Phys. Oceanogr.*, **17,** 1619–1626.

Ivchenko, V. O., A. M. Treguier, and S. E. Best, 1997: A kinetic energy budget and internal instabilities in the Fine Resolution Antarctic Model. *J. Phys. Oceanogr.*, **27,** 5–22.

Johns, W. E., 1988: One-dimensional baroclinic unstable waves on the Gulf Stream potential vorticity gradient near Cape Hatteras. *Dyn. Atmos. Oceans*, **11,** 323–350.

Killworth, P. D., 1980: Barotropic and baroclinic instability in rotating statified fluids. *Dyn Atmos. Oceans*, **4,** 143–184.

LeBlond, P. H., and L. A. Mysak, 1978: *Waves in the Ocean.* Elsevier.

Levitus, S., 1982: *Climatological Atlas of the World Ocean.* NOAA Prof. Paper No. 13, U.S. Govt. Printing Office 173 pp.

Lutjeharms, J. R. E., 1988: Remote sensing corroboration of the retroflection of the East Madagascar Current. *Deep-Sea Res.,* **35** (12), 2045–2050.

——, 1989: The role of mesoscale turbulence in the Agulhas Current system. *Mesoscale/Synoptic Coherent Structures in Geophysical Turbulence,* J. C. J. Nihoul and B. M. Jamart, Eds., Elsevier, 357–372.

——, 1996: The exchange of water between the South Indian and the South Atlantic Oceans. *The South Atlantic: Present and Past Circulation,* G. Wefer et al. Eds., Springer-Verlag, 125–162.

——, and A. L. Gordon, 1987: Shedding of an Agulhas ring observed at sea. *Nature,* **325,** 138–140.

——, and H. R. Roberts, 1988: The Natal Pulse: An extreme transient on the Agulhas Current. *J. Geophys. Res.,* **93,** 631–645.

——, and H. R. Valentine, 1988: Eddies at the subtropical convergence south of Africa. *J. Phys. Oceanogr.,* **18,** 761–774.

——, and R. C. van Ballegooyen, 1988a: The retroflection of the Agulhas Current. *J. Phys. Oceanogr.,* **18,** 1570–1583.

——, and ——, 1988b: Anomalous upstream retroflection in the Agulhas Current. *Science,* **240,** 1770–1772.

——, and A. D. Connell, 1989: The Natal Pulse and inshore counter currents off the South African east coast. *S. Afr. J. Sci.,* **85,** 533–535.

——, N. D. Bang, and C. P. Duncan, 1981: Characteristics of the currents east and south of Madagascar. *Deep-Sea Res.,* **28,** 879–899.

——, S. J. Weeks, R. C. van Ballegooyen, and F. A. Shillington, 1992: Shedding of an eddy from the seaward front of the Agulhas Current. *S. Afr. J. Sci.,* **88,** 430–433.

Miller, J. L., and T. N. Lee, 1995: Gulf Stream meanders in the South Atlantic Bight 1. Scaling and energetics *J. Geophys. Res.,* **100,** 6687–6704.

Naeije, M. C., K. F. Wakker, R. Scharroo, and B. A. C. Ambrosius, 1992: Observations of mesoscale ocean currents from GEOSAT altimeter data, ISPRS. *J. Photogramm. Remote Sens.,* **47,** 347–368.

Nof, D., 1986: The collision between the Gulf Stream and warm-core rings. *Deep-Sea Res.,* **33,** 359–378.

Olsen, D. B., and R. H. Evans, 1986: Rings of the Agulhas Current. *Deep-Sea Res.,* **33,** 27–42.

Ou, H. W., and W. P. M. de Ruijter, 1986: Separation of an inertial boundary current from a curved coastline. *J. Phys. Oceanogr.,* **16,** 280–289.

Pearce, A. F., 1977: Some features of the upper 500 m of the Agulhas Current. *J. Mar. Res.,* **35,** 731–753.

Pedlosky, J. 1964: The stability of currents in the atmosphere and the ocean: Part I. *J. Atmos. Sci.,* **21,** 201–219.

——, 1970: Finite-amplitude baroclinic waves. *J. Atmos. Sci.,* **27,** 15–30.

——, 1987: *Geophysical Fluid Dynamics.* Springer-Verlag, 710 pp.

Samelson, R. M., and J. Pedlosky, 1990: Local baroclinic instability of flow over variable topography. *J. Fluid Mech.,* **221,** 411–436.

Seatre, R., and A. Jorge da Silva, 1984: The circulation of the Mozambique Channel. *Deep-Sea Res.,* **31,** 485–508.

Steinsaltz, D., 1987: Instability of baroclinic waves with bottom slope. *J. Phys. Oceanogr.,* **17,** 2243–2350.

Toole, J. M., and M. E. Raymer, 1985: Heat and fresh water budgets of the Indian Ocean—Revisited. *Deep-Sea Res.,* **32,** 917–928.

Vazquez, J., E. Smith, M. Hamilton, A. van Tran, and R. Sumagaysay, 1994: NOAA/NASA AVHRR Pathfinder Ocean Project. PO-DAAC, Jet Propulsion Lab.

van Leeuwen, P. J., W. P. M. De Ruijter, and J. R. E. Lutjeharms, 1999: Natal Pulses and the formation of Agulhas rings. *J. Geophys. Res.,* in press.

Veronis, G., 1973: Model of the world ocean circulation I, Wind-driven two layer. *J. Mar. Res.,* **31,** 228–288.

Wakker, K. F., R. C. A. Zandbergen, M. C. Naeije, and B. A. C. Ambrosius, 1990: GEOSAT altimeter data analysis for the oceans aound South Africa. *J. Geophys. Res.,* **95,** 2991–3006.

Wisse, E., M. C. Naeye, R. Scharroo, A. J. E. Smith, F. C. Vossepoel, and K. F. Wakker 1995: Processing of ERS-1 and TOPEX/POSEIDON altimeter measurements. BCRS Rep. 95-02, BCRS study 1.2/OP-01, 146 pp. [Available from Netherlands Remote Sensing Board (BCRS), P. O. Box 5023, 2600 GA Delft, Netherlands.]